The benefits of combined therapy, such as photodynamic therapy and anti-VEGF antibody, have been discussed.[27]

In conclusion, intravitreal vasohibin-1 in monkey eyes is safe and can reduce the activity of laser-induced CNVs and thus preserve the function of the macula.

Key words: choroidal neovascularization, laser-induced, monkey, vascular endothelial growth factor, vasohibin-1.

References

1. Klein R, Peto T, Bird AC, Vannewkirk MR. The epidemiology of age-related macular degeneration. Am J Ophthalmol 2004; 137:486–495.
2. Bressler NM, Bressler SB, Fine SL. Age-related macular degeneration. Surv Ophthalmol 1998;32:375–413.
3. Argon laser photocoagulation for neovascular maculopathy. Three-year results from randomized clinical trials Macular Photocoagulation Study Group. Arch Ophthalmol 1986;104: 694–701.
4. Thomas MA, Grand MG, Williams DF, et al. Surgical management of subfoveal choroidal neovascularization. Ophthalmology 1992;99:952–968.
5. Eckardt C, Eckardt U, Conrad HG. Macular rotation with and without counter-rotation of the globe in patients with age-related macular degeneration. Graefes Arch Clin Exp Ophthalmol 1999;237:313–325.
6. Reichel E, Berrocal AM, Ip M, et al. Transpupillary thermotherapy of occult subfoveal choroidal neovascularization in patients with age-related macular degeneration. Ophthalmology 1999; 106:1908–1914.
7. Photodynamic therapy of subfoveal choroidal neovascularization in age-related macular degeneration with verteporfin: one year results of 2 randomized clinical trials-TAP report Treatment of Age-related Macular Degeneration with Photodynamic Therapy (TAP). Study Group. Arch Ophthalmol 1999;117:1329–1345.
8. Grisanti S, Tatar O. The role of vascular endothelial growth factor and other endogenous interplayers in age-related macular degeneration. Prog Retin Eye Res 2008;27:372–390.
9. Miller JW, Adamis AP, Shima DT, et al. Vascular endothelial growth factor/vascular permeability factor is temporally and spatially correlated with ocular angiogenesis in a primate model. Am J Pathol 1994;145:574–584.
10. Krzystolik MG, Afshari MA, Adamis AP, et al. Prevention of experimental choroidal neovascularization with intravitreal anti-vascular endothelial growth factor antibody fragment. Arch Ophthalmol 2002;120:338–346.
11. Rosenfeld PJ, Brown DM, Heier JS, et al. Ranibizumab for neovascular age-related macular degeneration. N Engl J Med 2006;355:1419–1431.
12. Pilli S, Kotsolis A, Spaide RF, et al. Endophthalmitis associated with intravitreal anti-vascular endothelial growth factor therapy injections in an office setting. Am J Ophthalmol 2008;145:879–882.
13. Lux A, Llacer H, Heussen FMA, Joussen AM. Non-responders to bevacizumab (Avastin) therapy of choroidal neovascular lesions. Am J Ophthalmol 2007;91:1318–1322.
14. Watanabe K, Hasegawa Y, Yamashita H, et al. Vasohibin as an endothelium-derived negative feedback regulator of angiogenesis. J Clin Invest 2004;114:898–907.
15. Shimizu K, Watanabe K, Yamashita H, et al. Gene regulation of a novel angiogenesis inhibitor, vasohibin, in endothelial cells. Biochem Biophys Res Commun 2005;327:700–706.
16. Shen J, Yang X, Xiao WH, et al. Vasohibin is up-regulated by VEGF in the retina and suppresses VEGF receptor 2 and retinal neovascularization. FASEB J 2006;20:723–725.
17. Sato H, Abe T, Wakusawa R, et al. Vitreous levels of vasohibin-1 and vascular endothelial growth factor in patients with proliferative diabetic retinopathy. Diabetologia 2009;52:359–361.
18. Wakusawa R, Abe T, Sato H, et al. Expression of vasohibin, an antiangiogenic factor, in human choroidal neovascular membranes. Am J Ophthalmol 2008;146:235–243.
19. Wakusawa R, Abe T, Sato H, et al. Suppression of choroidal neovascularization by vasohibin-1, vascular endothelium-derived angiogenic inhibitor. Invest Ophthalmol Vis Sci 2011;52:3272–3280.
20. Tobe T, Ortega S, Luna JD, et al. Targeted disruption of the FGF2 gene does not prevent choroidal neovascularization in a murine model. Am J Pathol 1998;153:1641–1646.
21. Heishi T, Hosaka T, Suzuki Y, et al. Endogenous angiogenesis inhibitor vasohibin1 exhibits broad-spectrum antilymphangiogenic activity and suppresses lymph node metastasis. Am J Pathol 2010;176:1950–1958.
22. Krzystolik MG, Afshari MA, Adamis AP, et al. Prevention of experimental choroidal neovascularization with intravitreal anti-vascular endothelial growth factor antibody fragment. Arch Ophthalmol 2002;120:338–346.
23. Miyake Y, Yanagida K, Yagasaki K, et al. Subjective scotometry and recording of local electroretinogram and visual evoked response. System with television monitor of the fundus. Jpn J Ophthalmol 1981;25:439–448.
24. Kondo M, Ueno S, Piao CH, et al. Comparison of focal macular cone ERGs in complete-type congenital stationary night blindness and APB-treated monkeys. Vision Res 2008;48: 273–280.
25. Hogan MJ, Kimura SJ, Thygeson P. Signs and symptoms of uveitis. I. Anterior uveitis. Am J Ophthalmol 1959;47:155–170.
26. Zhang M, Zhang J, Yan M, et al. Recombinant anti-vascular endothelial growth factor fusion protein efficiently suppresses choroidal neovascularization in monkeys. Mol Vision 2008;14:37–49.
27. Husain D, Kim I, Gauthier D, et al. Safety and efficacy of intravitreal injection of ranibizumab in combination with verteporfin PDT on experimental choroidal neovascularization in the monkey. Arch Ophthalmol 2005;123:509–516.
28. Shen WY, Lee SY, Yeo I, et al. Predilection of the macular region to high incidence of choroidal neovascularization after intense laser photocoagulation in the monkey. Arch Ophthalmol 2004;122:353–360.
29. Hosaka T, Kimura H, Heishi T, et al. Vasohibin-1 expression in endothelium of tumor blood vessels regulates angiogenesis. Am J Pathol 2009;175:430–439.
30. Zhou SY, Xie ZL, Xiao O, et al. Inhibition of mouse alkali burn induced-corneal neovascularization by recombinant adenovirus human vasohibin-1. Mol Vision 2010;16:1389–1398.
31. Alon T, Hemo I, Itin A, et al. Vascular endothelial growth factor acts as a survival factor for newly formed retinal vessels and has implications for retinopathy of prematurity. Nat Med 1995;1:1024–1028.

Chapter 40
Vasohibin-1 and Retinal Pigment Epithelium

Yumi Ishikawa, Nobuhiro Nagai, Hideyuki Onami, Norihiro Kumasaka, Ryosuke Wakusawa, Hikaru Sonoda, Yasufumi Sato, and Toshiaki Abe

Keywords Vasohibin • VEGF • Retinal pigment epithelium • Hypoxia • Cell dynamics • Cobalt chloride

40.1 Introduction

Choroidal neovascularization (CNV) leads to subretinal hemorrhages, exudative lesions, serous retinal detachment, and disciform scars in patients with age-related macular degeneration (AMD) (Bressler et al. 1998). Vascular endothelial growth factor (VEGF), a pro-angiogenic factor, plays a major role in the development of CNV (Spilsbury et al. 2000). Recently, anti-VEGF treatment for patients with AMD has developed and reported good results (Krzystolik et al. 2002; Rosenfeld et al. 2006). However, there are many problems, such as repeated intravitreal injections, side effects (Pilli et al. 2008), suppression of the important physiological VEGF function (Alon et al. 1995), and further not all patients respond well to this therapy (Lux et al. 2007). Vasohibin-1 is a VEGF-inducible gene in human cultured endothelial cells (ECs) with antiangiogenic properties (Watanabe et al. 2004; Sonoda et al. 2006). Vasohibin-1 is induced by several pro-angiogenic factors such as VEGF and

Y. Ishikawa • N. Nagai • H. Onami • N. Kumasaka • R. Wakusawa • T. Abe (✉)
Division of Clinical Cell Therapy, United Center for Advanced Research and Translational Medicine (ART), Tohoku University Graduate School of Medicine, 1-1 Seiryoumachi Aobaku Sendai, Miyagi, Japan
e-mail: toshi@oph.med.tohoku.ac.jp

H. Sonoda
Discovery Research Laboratories, Shionogi and Co. Ltd, Osaka, Japan

Y. Sato
Department of Vascular Biology, Institute of Development, Aging, and Cancer, Tohoku University Graduate School of Medicine, Miyagi, Japan

M.M. LaVail et al. (eds.), *Retinal Degenerative Diseases*, Advances in Experimental Medicine and Biology 723, DOI 10.1007/978-1-4614-0631-0_40,

basic fibroblast growth factor (bFGF) (Watanabe et al. 2004). We showed that the vasohibin-1/VEGF ratio might play a role for clinical significance of CNV in patients with AMD using surgically excised CNV membranes (Wakusawa et al. 2008). The membranes included not only ECs but also retinal pigment epithelium (RPE). In this report, we examined the effects of vasohibin-1 on RPE.

40.2 Methods

40.2.1 RPE Preparation

We used commercially available rat RPE cell line, RPE-J. RPE-J was cultured in DMEM/F-12 medium with 4% fetal bovine serum (FBS; Sigma, St. Louis MO) with 5% CO_2 supply at 33°C. Human vasohibin-1 cDNA with antineomycin gene vector was transduced into RPE-J as we previously reported (Abe et al. 2008). Cells that were stably introduced the vector were selected by antibiotics. We selected 18 clones on both vasohibin-1 cDNA and only vector-transduced RPE-Js. Cobalt chloride (100–300 μM) and low glucose (0–100 μM) and oxygen supply (2%) were used for hypoxic stress. Vasohibin-1 was supplied from Shionogi and Co. Ltd, Osaka, Japan and VEGF and other chemicals were purchased from Wako (Tokyo Japan).

40.2.2 Real-Time RPE Impedance Analysis and MTS Assay

Dynamic cellular biology of the cultured RPE was monitored using Real-Time Cell Analyzer (RTCA), xCELLigence System (Roche Applied Science, Mannheim, Germany). The system evaluates cellular events in real time measuring electrical impedance at an electrode/solution interface at the bottom of cell culture plates. The system provides cell number, viability, morphology, and adhesion described as Cell Index (CI). RPE proliferation was also evaluated by 3-(4, 5-dimethylthiazol-2-yl)-5-(3-carboxymethoxyphenyl)-2-(4-sulfophenyl)-2H-tetrazolium, inner salt (MTS) assay, and counting cell number for each condition.

40.2.3 Extraction of mRNA, cDNA Generation, Reverse-Transcriptase, and Real-Time Polymerase Chain Reaction (RT-PCR)

mRNA was extracted and cDNAs were generated from the cells according to the manufacturer's instructions (Pharmacia Biotech Inc., Uppsala, Sweden). Semiquantitative real-time PCR was carried out by the primer sets described below (LightCycleST300:Roche, Basel, Swiss). The sequences were 5′-TCT GCT CTC

TTG GGT GCA AT-3′and 5′-TTC CGG TGA GAG GTC CGG TT-3′ for VEGF, 5′-GAT TCC CAT ACC AAG TGT GCC-3′ and 5′-ATG TGG CGG AAG TAG TTC CC-3′for vasohibin-1, and 5′-CATCACCATCTTCCAGGAGC-3′ and 5′-CATGAGTCCTTCCACGATACC-3′ for GAPDH. All data were normalized to the GAPDH expression level, thus giving the relative expression level.

40.2.4 Western Blot Analysis for Vasohibin-1 and VEGF

Cells were collected and used for western blotting analysis after sonication, as we reported previously (Abe et al. 2008). Cells were washed in ice-cold Dalbecco's phosphate buffered saline (DPBS) 3 times, and then immediately sonicated in lysis buffer. After blotting on Immune-Blot PVDF Membrane (BIO-RAD Laboratories, CA), it was incubated overnight in mouse antivasohibin-1 or anti-VEGF antibody (Santa Cruz) at 4°C and visualized using an enhanced chemiluminescence system (ECL Plus, GE Healthcare) according to the manufacturer's instructions.

40.3 Results

40.3.1 Vasohibin-1 Expression

Vasohibin-1 expression in the RPE was confirmed by real-time PCR and western blot analysis. When we cultured the cells with cobalt chloride, a pseudo-hypoxic condition, or low oxygen (2%), 1% serum, and no glucose, gradual upregulation of VEGF gene was observed with 100-μM cobalt chloride (Fig. 40.1a). Conversely, statistically significant low vasohibin-1 expression was observed with 100-μM cobalt chloride at more than 12-h culture when compared to those of standard culture or less than 6-h culture (Fig. 40.1b). Western blot analysis showed that vasohibin-1 expression seemed to be downregulated at more than 36-h culture with 100-μM cobalt chloride (Fig. 40.1c).

40.3.2 RPE Dynamics and Proliferation by Vasohibin-1

An RTCA was used to monitor dynamic changes in the properties of RPE cells during the culture. The parameter of CI shows cell viability, number, morphology, and adhesion to the bottom of the plates. When we cultured the cells under standard condition as described above, we found no difference of CI even though we added VEGF (Fig. 40.2a) and/or vasohibin-1 (Fig. 40.2b). When we added VEGF (0.2–10 nM) in the culture medium at 2% oxygen, 1% serum, and no glucose, we found that VEGF enhanced CI (Fig. 40.2c). Statistically significant difference was observed when we cultured the cells more than 15 h after treatments with 1 and 2-nM VEGF.

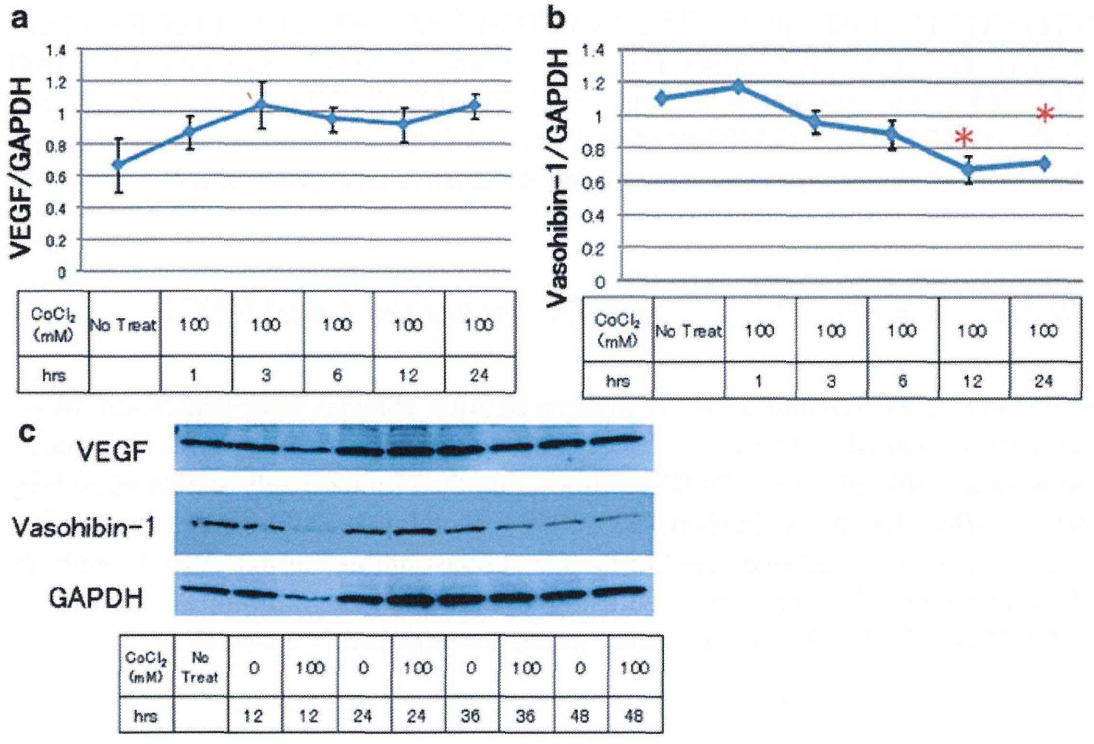

Fig. 40.1 Real-time PCR of VEGF (**a**) and vasohibin-1 (**b**) genes is shown. VEGF gene was upregulated in RPE-J with cobalt chloride during successive culture whereas vasohibin-1 gene was suppressed. Western blot analysis (**c**) shows decreased vasohibin-1 expression at the condition

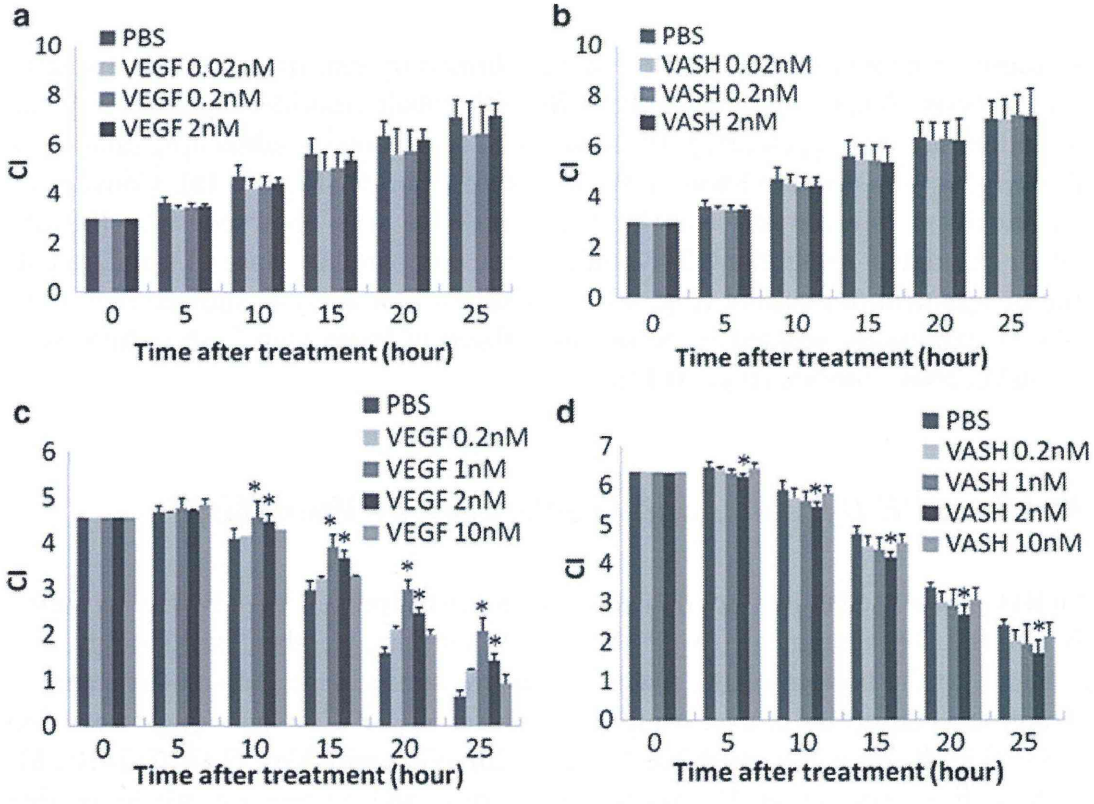

Fig. 40.2 Cell Index of RTCA shows that VEGF enhanced CI at hypoxic condition (**a**), conversely vasohibin-1 reduced CI only at hypoxic condition (**b**). The results were not observed at normal condition

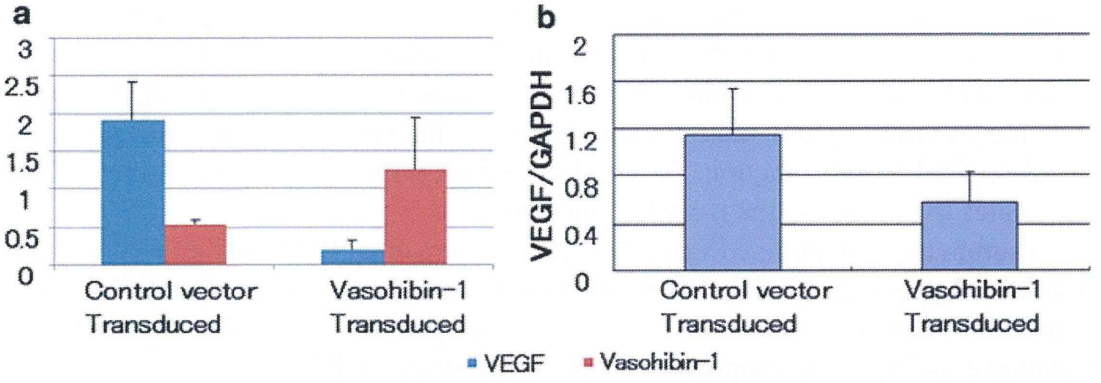

Fig. 40.3 Human vasohibin-1 gene was transduced into RPE-J. We selected 18 clones on both vasohibin-1 gene transduced and only vector-transduced RPE-J. Statistically significant less VEGF gene expression was observed in vasohibin-1 gene-transduced cDNA when compared to that of vector-transduced cDNA (**a**). Western blot analysis also showed comparable results (**b**)

Conversely, when we applied vasohibin-1 (0.2–10 nM) in the culture medium at 2% oxygen, 1% serum, and no glucose, we found that vasohibin-1 showed lower CI (Fig. 40.2d). Statistically significant difference was observed at 2-nM vasohibin-1. Vasohibin-1 application also showed statistically significant small cell number either 300-μM cobalt chloride or 2% oxygen, 1% serum, and no glucose. When we performed MTS assay, statistically significant less cell proliferation was also observed at these indicated conditions. When we examined the apoptotic cells, there was no significant difference. Human vasohibin-1 gene-transduced RPE-J showed statistically significant less VEGF expression when compared to those of vector-transduced cell by real-time PCR and western blot analysis (Fig. 40.3a, b).

40.4 Discussion

Vasohibin-1 is an endogenous antiangiogenic agent that is induced by variable pro-angiogenic factors such as VEGF and bFGF. Vasohibin-1 was reported to inhibit the sprouting of new vessels and to support vascular maturation processes (Kimura et al. 2009). These antiangiogenic properties were detected after recombinant vasohibin-1 was used for corneal and retinal neovascularization (Watanabe et al. 2004). We have found that vasohibin-1 is expressed on ECs of choroidal and retinal vessels, human CNV membranes (Wakusawa et al. 2008), and proliferative membranes of diabetic retinopathy (Sato et al. 2009). In addition, we suggested that the vasohibin-1/VEGF ratio was related to the activity of the CNV (Wakusawa et al. 2008). RPE is known for secreting VEGF from its basal side to choriocapillaris direction and performs important function for the survival of the vascular ECs and nonvascular cells developmentally and also in adults (Alon et al. 1995). This mechanism also maintains low VEGF concentration at subretinal space (Peng et al. 2010). Because of this specific function, we examined the correlation of vasohibin-1 and VEGF on RPE. From the results of present study, vasohibin-1 was expressed in RPE and the

expression was suppressed under hypoxic condition in RPE-J. Vasohibin-1 was also suspected to inhibit VEGF function of rat RPE. Interestingly, these results were observed only at hypoxic conditions and not in standard culture condition. Together with the previous reports, these results may show that vasohibin-1 may not suppress physiological VEGF function. External vasohibin-1 may participate as one of the molecules that suppress the pathological CNV.

In summary, we examined vasohibin-1 expression in rat RPE and the effects under normal or hypoxic condition. Vasohibin-1 expression was suppressed under hypoxic conditions. External vasohibin-1 plays an important role on RPE, especially in hypoxic condition, and suppresses VEGF function on rat RPE.

Acknowledgments This study was supported in part by grants from Grants-in-Aid for Scientific Research 20592030, 21592214 from the Japan Society for the Promotion of Science, Chiyoda-ku, Tokyo, Japan and Suzuken Memorial Foundation.

References

Abe T, Wakusawa R, Seto H et al (2008) Topical doxycycline can induce expression of BDNF in transduced retinal pigment epithelial cells transplanted into the subretinal space. Invest Ophthalmol Vis Sci 49: 3631–3639

Alon T, Hemo I, Itin A et al (1995) Vascular endothelial growth factor acts as a survival factor for newly formed retinal vessels and has implications for retinopathy of prematurity. Nat Med 1: 1024–1028

Bressler NM, Bressler SB, Fine SL (1998) Age-related macular degeneration. Surv Ophthalmol 32: 375–413

Kimura H, Miyashita H, Suzuki Y et al (2009) Distinctive localization and opposed roles of vasohibin-1 and vasohibin-2 in the regulation of angiogenesis. Blood 113: 4810–4818

Krzystolik MG, Afshari MA, Adamis AP et al (2002) Prevention of experimental choroidal neovascularization with intravitreal anti-vascular endothelial growth factor antibody fragment. Arch Ophthalmol 120: 338–346

Lux A, Llacer H, Heussen FMA et al (2007) Non-responders to bevacizumab (Avastin) therapy of choroidal neovascular lesions. Am J Ophthalmol 91: 1318–1322

Peng S, Adelman RA, Rizzolo LJ (2010) Minimal effects of VEGF and anti-VEGF drugs on the permeability or selectivity of RPE tight junctions. Invest Ophthalmol Vis Sci 51: 3216–33225

Pilli S, Kotsolis A, Spaide RF et al (2008) Endophthalmitis associated with intravitreal anti-vascular endothelial growth factor therapy injections in an office setting. Am J Ophthalmol 145: 879–882

Rosenfeld PJ, Brown DM, Heier JS et al (2006) MARINA Study Group. Ranibizumab for neovascular age-related macular degeneration. N Engl J Med 355: 1419–1431

Sato H, Abe T, Wakusawa R et al (2009) Vitreous levels of vasohibin-1 and vascular endothelial growth factor in patients with proliferative diabetic retinopathy. Diabetologia 52: 359–361

Sonoda H, Ohta H, Watanabe K et al (2006) Multiple processing forms and their biological activities of a novel angiogenesis inhibitor vasohibin. Biochem Biophys Res Commun 342: 640–646

Spilsbury K, Garrett KL, Shen WY et al (2000) Overexpression of vascular endothelial growth factor (VEGF) in the retinal pigment epithelium leads to the development of choroidal neovascularization. Am J Pathol 157: 135–144

Wakusawa R, Abe T, Sato H et al (2008) Expression of vasohibin, an antiangiogenic factor, in human choroidal neovascular membranes. Am J Ophthalmol 146: 235–243

Watanabe K, Hasegawa Y, Yamashita H et al (2004) Vasohibin as an endothelium-derived negative feedback regulator of angiogenesis. J Clin Invest 114: 898–907

Experimental Eye Research 108 (2013) 10–15

Contents lists available at SciVerse ScienceDirect

Experimental Eye Research

journal homepage: www.elsevier.com/locate/yexer

Comparison of CCD-equipped laser speckle flowgraphy with hydrogen gas clearance method in the measurement of optic nerve head microcirculation in rabbits

Hiroaki Takahashi [a], Tetsuya Sugiyama [b,*], Hideki Tokushige [a], Takatoshi Maeno [c], Toru Nakazawa [d], Tsunehiko Ikeda [b], Makoto Araie [e]

[a] Research Laboratory for Drug Development, Senju Pharmaceutical Co., Ltd., 1-5-4 Murotani, Nishi-ku, Kobe, Hyogo 651-2241, Japan
[b] Department of Ophthalmology, Osaka Medical College, 2-7 Daigaku-machi, Takatsuki, Osaka 569-8686, Japan
[c] Department of Ophthalmology, Toho University Sakura Medical Center, 564-1 Shimoshizu, Sakura, Chiba 285-8741, Japan
[d] Department of Ophthalmology, Tohoku University Graduate School of Medicine, 1-1 Seiryo-machi, Aoba-ku, Sendai, Miyagi 980-8574, Japan
[e] Kanto Central Hospital of The Mutual Aid Association of Public School Teachers, 6-25-1 Kamiyoga, Setagaya-ku, Tokyo 158-0098, Japan

ARTICLE INFO

Article history:
Received 6 October 2012
Accepted in revised form 10 December 2012
Available online 19 December 2012

Keywords:
optic nerve head
laser speckle flowgraphy
mean blur rate
hydrogen gas clearance method
capillary blood flow
rabbit

ABSTRACT

The aim of this study was to verify the correlation between mean blur rate (MBR) obtained with CCD-equipped laser speckle flowgraphy (LSFG) and capillary blood flow (CBF) obtained by the hydrogen gas clearance method in rabbit optic nerve head (ONH). Using Japanese white rabbits under systemic anesthesia, a hydrogen electrode was inserted an area of the ONH free from superficial capillaries. MBR was measured with LSFG near the hydrogen electrode. CBF and MBR were measured in the range of 32.4–83.5 mL/min/100 g and 3.5–6.0, respectively. MBR and CBF were significantly correlated ($r = 0.73$, $P < 0.01$, $n = 14$). After inhalation of carbon dioxide (CO_2) or intravenous administration of endothelin-1 (ET-1), MBR and CBF were changed in the relative range of 0.74–1.27 and 0.76–1.35, respectively. The relative changes in MBR and CBF induced by CO_2 and ET-1 were also significantly correlated ($r = 0.67$, $P < 0.01$). The current results suggest that MBR may correlate with CBF and also change with CBF, as an index of blood flow in the ONH, linearly.

1. Introduction

Abnormal blood flow regulation is widely recognized to contribute to the pathophysiology of ocular diseases such as glaucoma (Grieshaber et al., 2007; Moore et al., 2008; Pemp et al., 2009). Circulatory factors in the retrobulbar arteries may be associated with the progression of visual field defects in patients with normal-tension glaucoma (Yamazaki and Drance, 1997). Progressive structural changes in the optic nerve head (ONH) also have been related to abnormal ocular blood flow in glaucoma patients (Harris et al., 2008b). For example, Logan et al. (2004) found lower levels of retinal blood flow in abnormal segments of the ONH than in a corresponding normal segment in glaucoma patients. In addition, glaucoma patients with normal rim segments demonstrated lower retinal blood flow than controls at each location sampled. However, the role played by blood flow and ischemia on the ONH and retina in glaucoma has not yet been clarified, in part because technical difficulties have limited the accurate measurement of ocular blood flow in relevant vascular beds (Caprioli and Coleman, 2010; Harris et al., 2008a).

The Association for Ocular Circulation (http://www.obfra.org/) has published consensus reports on ocular circulation measurement methods such as laser Doppler flowmetry (Riva et al., 2010), laser speckle flowgraphy (LSFG) (Sugiyama et al., 2010), retinal vessel analysis (Garhofer et al., 2010), and color Doppler imaging (Stalmans et al., 2011). Among them, LSFG is the only method available to measure tissue circulation non-invasively and provide a 2-dimensional map of ocular tissue circulation. Normalized blur (NB) was the value used previously in LSFG and represents an index of blood velocity (Tamaki et al., 1994, 1995). *In vitro*, NB demonstrated a good linear correlation with the mean velocity of blood cells flowing through a glass capillary tube (calculated from the blood flow rate generated by a calibrated peristaltic pump) (Nagahara et al., 1999) and with the speed of rotation of a ground-

Abbreviations: CBF, capillary blood flow; LSFG, laser speckle flowgraphy; MBR, mean blur rate; ONH, optic nerve head.

* Corresponding author. Tel.: +81 72 683 1221; fax: +81 72 681 8195.
E-mail addresses: tsugiyama@poh.osaka-med.ac.jp, tsugiyama7@gmail.com (T. Sugiyama).

0014-4835/$ – see front matter © 2012 Elsevier Ltd. All rights reserved.
http://dx.doi.org/10.1016/j.exer.2012.12.003

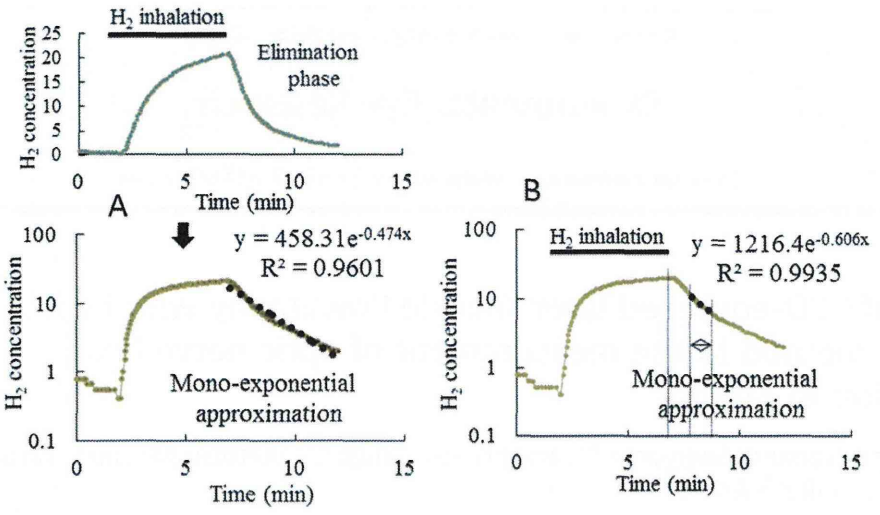

Fig. 1. An example of analyzing hydrogen clearance curve to obtain capillary blood flow (CBF) by the hydrogen gas clearance method. The hydrogen concentration was plotted into logarithm (A). The half-life ($T_{1/2}$) at 1–2 min after stopping hydrogen inhalation was adopted for calculation because the linearity of hydrogen clearance in logarithm was the highest there (B). We then calculate CBF as $69.3/T_{1/2}$ (ml/min/100 g).

glass disc (calculated from the velocity of diffusing particles, which are models of blood cells, on the glass) (Nagahara et al., 1999; Tamaki et al., 1994, 1995,). *In vivo*, NB was well correlated with tissue blood flow rates determined using the microsphere method in the retina, choroid, or iris, as well as blood flow rates determined with the hydrogen gas clearance method in the ONH (Sugiyama et al., 1996; Takayama et al., 2003; Tamaki et al., 1994, 1995, 1996, 2003; Tomidokoro et al., 1998; Tomita et al., 1999).

In 2008, LSFG-NAVI™ was approved as a medical apparatus by the Pharmaceuticals and Medical Devices Agency in Japan. It has adopted a new index: mean blur rate (MBR), the relative velocity index of erythrocytes (Konishi et al., 2002; Watanabe et al., 2008). Recently, Aizawa et al. (2011) reported that MBR has high reproducibility in normal and glaucoma subjects. However, no reports to date have investigated whether MBR is correlated with blood flow rate in the ONH.

The hydrogen gas clearance technique provides multiple capillary blood flow (CBF) measurements quantitatively over long periods of time (Aukland et al., 1964; Csete et al., 2004; Srinivasan et al., 2011). In the ophthalmic field, this technique has been applied to the ONH in rhesus monkeys (Ernest, 1976) and demonstrated high reproducibility in the measurement of CBF in rabbit ONH (Sugiyama et al., 1995). However, use of this technique is limited to laboratory research because it is highly invasive. The aim of the current study was to verify the correlation between MBR obtained by LSFG and CBF obtained by the hydrogen gas clearance method in the rabbit ONH.

2. Materials and methods

2.1. Animals

Eighteen male Japanese white rabbits weighing 2.5–3.3 kg were purchased from Kitayama Lab. (Nagano, Japan) for the current study. They were housed in an air-conditioned room at temperature of 23 ± 3 °C and humidity of 55 ± 10% with a 12-h light–dark cycle and provided with tap water *ad libitum* throughout the experimental period. All animal studies were performed in accordance with the ARVO statement for the use of animals in ophthalmic and vision research and with the approval of the Institutional Animal Care and Use Committee of Kobe Creative Center, Senju Pharmaceutical Co., Ltd.

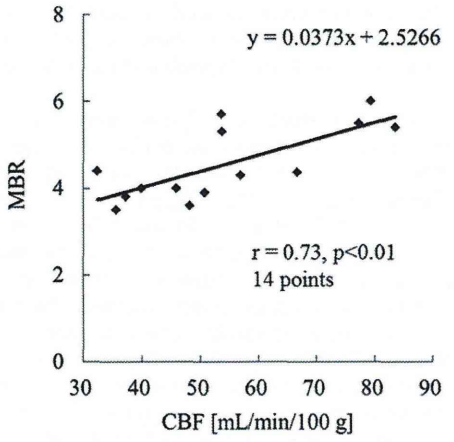

Fig. 2. Correlation between the absolute values of CBF and MBR at baseline. CBF and MBR were obtained by the hydrogen gas clearance method and LSFG, respectively. Each point represents 1 of 14 different rabbits. Correlation coefficient (r) was 0.73 ($P < 0.01$).

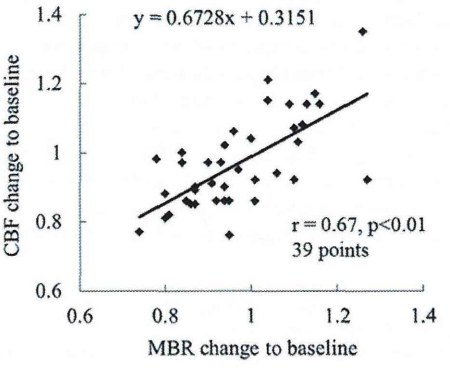

Fig. 3. Correlation between the relative changes in CBF and MBR after treatment with CO_2 and ET-1. Each point represents the ratio of relative values to baseline values. Total points were obtained from 39 time points ($n = 9$ and 6 for CO_2 and ET-1, respectively) in 10 eyes of 14 rabbits. Correlation coefficient (r) was 0.67 ($P < 0.01$).

Table 1
Distributions of variances by randomized block ANOVA regarding individuality and time-course changes after each treatment.

Treatment	Individuality		Time-course changes	
	CBF	MBR	CBF	MBR
CO_2	569.268 (8)*	15.046 (8)*	68.750 (3)*	1.358 (3)*
ET-1	262.346 (5)*	1.834 (5)*	11.056 (2)	0.127 (2)

Asterisks represent significant differences ($P < 0.05$) among values obtained from individual rabbits or values at different time points. Degrees of freedom were shown in parentheses.

2.2. Measurement of CBF in ONH

Mydriasis was induced by topical tropicamide (Mydrin®-M ophthalmic solution 0.4%, Santen Pharmaceutical Co. Ltd., Osaka, Japan). Animals were anesthetized by intraperitoneal injection of 0.8 mg/kg urethane at 0.4 g/mL (Nakalai, Kyoto, Japan) and additional intramuscular injection of 0.1 mg/kg urethane as necessary. Topical anesthesia was induced by topical oxybuprocaine (Benoxil® ophthalmic solution 0.4%, Santen Pharmaceutical Co. Ltd.). The CBF in the ONH was measured by the hydrogen gas clearance method as previously reported (Sugiyama et al., 1996). A hydrogen electrode (Cat.# OA211-013, platinum needle with a 0.7-mm long and 0.1-mm diameter Pt–Ir tip, Unique Medical Co., Ltd., Tokyo, Japan) was inserted into a lower portion of the ONH with no visible surface vessels through the vitreous body from the pars plana using a vitrectomy lens. The reference electrode was subcutaneously fixed on the head. After the inhalation of 10% hydrogen gas by a mask at 5 L/min for 5 min, CBF was calculated with the hydrogen concentration half-life ($T_{1/2}$) using a hydrogen clearance flow meter (model MDH-D1, Unique Medical Co., Ltd.). As shown in Fig. 1A, since the clearance curve is approximately mono-exponential, the hydrogen concentration was plotted into logarithm to get half-life ($T_{1/2}$) for calculation. Specifically in the current study, the linearity of hydrogen clearance in logarithm was found beforehand to be the highest at 1–2 min after stopping hydrogen inhalation (Fig. 1B), therefore we adopted the half-life there to calculate CBF as $69.3/T_{1/2}$ (mL/min/100 g).

2.3. Measurement method of MBR in ONH

MBR was measured with a LSFG-NAVI-MRC™ device (Softcare Ltd., Iizuka, Japan). The LSFG-NAVI-MRC™ consisted of a fundus camera equipped with a diode laser (wavelength: 830 nm) and a CCD image sensor (750 × 360 pixels). The principle and application of this method have been described previously (Konishi et al., 2002; Sugiyama et al., 2010; Tamaki et al., 1995). The measurement area of MBR was designated as a square area free of visible surface vessels near the hydrogen electrode in the ONH.

2.4. Measurements of CBF and MBR before and after altering ONH blood flow

To check their stability in measuring ONH blood flow, CBF and MBR were recorded 3 times at 15-min intervals and 5 times at 5-min intervals, respectively. The intervals were recommended in previous reports (Sugiyama and Azuma, 1995; Tamaki et al., 1995). The inclusion criterion for the stability of measurements was a coefficient of variance (CV) of CBF within 0.1. Averages of measurement values were adopted as baseline values. The correlation between the baseline values of CBF and MBR was estimated. Baseline values were measured before the inhalation of carbon dioxide (CO_2) or intravenous administration of endothelin-1 (ET-1).

Immediately, 15, and 30 min after 5-min inhalation of 10% CO_2 in ordinary air via mask at 5 L/min, CBF and MBR were measured simultaneously in the same rabbit. CBF was measured once at each time point. MBR was recorded 5 times at each time point, and then the mean value was calculated. Human ET-1 (Peptide Institute, Osaka, Japan) was dissolved in 0.1% aqueous acetic acid to provide a 10^{-4} mol/L concentration and diluted with saline for a 10^{-6} mol/L solution. CBF and MBR were measured, as above, at 30 min and 1 h after intravenous injection (10^{-10} mol/kg) of the prepared ET-1 solution. The relative change in CBF and MBR was calculated by dividing by the baseline value. The expiratory CO_2 density and arterial O_2 and CO_2 pressure were not monitored.

2.5. Statistical analysis

Correlation analysis between CBF and MBR was performed using Ekuseru-Toukei 2008 statistical software (Social Survey Research Information Co., Ltd., Tokyo, Japan). We analyzed the effects of each treatment (namely, CO_2 and ET-1) on MBR and CBF by randomized block ANOVA with individual animals as a block using JMP software (Ver. 9.0.0, SAS Institute, Cary, NC). Findings of $P < 0.05$ were considered significant.

3. Results

3.1. Correlation between the baseline values of CBF and MBR

A plot of baseline CBF and MBR values is shown in Fig. 2. In 17 of 18 rabbits, the CV of CBF was within 0.1. For measurement of MBR in 3 of 17 rabbits, the square area could not be designated free from visible surface vessels near the hydrogen electrode in the ONH. Therefore, data from 14 eyes of 14 rabbits were used for this analysis. CBF and MBR were measured in the range (mean ± SE) of 32.4–83.5 (54.3 ± 4.5) mL/min/100 g and 3.5–6.0 (4.6 ± 0.2), respectively. A significant positive correlation between the absolute CBF and MBR baseline values was observed ($r = 0.73$, $P < 0.01$, $n = 14$).

3.2. Correlation between the relative change in CBF and MBR induced by inhalation of CO_2 and intravenous administration of ET-1

CBF was altered after inhalation of CO_2 or intravenous administration of ET-1. Relative values of CBF changed in the range of 0.74–1.27. MBR in the ONH was also altered. Relative values of MBR changed in the range of 0.76–1.35. A plot of relative changes in CBF and MBR is shown in Fig. 3. In 10 of 14 rabbits, the changes in CBF and MBR induced by CO_2 ($n = 9$) and ET-1 ($n = 6$) were measured with the hydrogen gas clearance method and LSFG, respectively. The relative changes in CBF and MBR demonstrated a significant positive correlation ($r = 0.67$, $P < 0.01$).

Table 2
Average changes in CBF and MBR after inhalation of CO_2.

	Baseline levels	Immediately	15 min	30 min
CBF (mL/min/100 g)	50.7 ± 11.5	52.3 ± 12.1 (1.04 ± 0.11)	48.3 ± 14.2 (0.95 ± 0.14)	46.0 ± 11.4* (0.91 ± 0.10)
MBR	4.7 ± 2.0	5.0 ± 2.0* (1.08 ± 0.10)	4.6 ± 2.5 (0.97 ± 0.13)	4.0 ± 1.4* (0.89 ± 0.08)

Data are expressed as mean ± SD for 9 rabbits. Asterisks represent significant differences ($P < 0.05$) compared to baseline levels by paired t-test. CBF/MBR changes to baseline levels were shown in parentheses.